

Probing Vortices in ^4He Nanodroplets

Francesco Ancilotto

*INFN, Udr Padova and DEMOCRITOS National Simulation Center, Trieste, Italy
and Dipartimento di Fisica “G. Galilei,” Università di Padova, via Marzolo 8, I-35131 Padova, Italy*

Manuel Barranco and Martí Pi

*Departament E.C.M., Facultat de Física, Universitat de Barcelona, E-08028, Spain
(Received 30 May 2003; published 5 September 2003)*

We present static and dynamical properties of linear vortices in ^4He droplets obtained from density functional calculations. By comparing the adsorption properties of different atomic impurities embedded in pure droplets and in droplets where a quantized vortex has been created, we suggest that Ca atoms should be the dopant of choice to detect vortices by means of spectroscopic experiments.

DOI: 10.1103/PhysRevLett.91.105302

PACS numbers: 67.40.Vs, 67.40.Fd, 67.40.Yv

The unique environment realized in liquid ^4He clusters has opened up, in recent years, new opportunities for atomic/molecular spectroscopy to probe superfluid phenomena on the atomic scale [1,2]. Helium droplets represent ideal nanoscale cryostats for a variety of fundamental experiments on liquid ^4He , including the study of quantized vortices [3]. Vortices, while energetically unfavorable [4], can potentially be stabilized by atomic or molecular impurities [5].

During the free jet expansion experiments described in Refs. [1,3], it is plausible that quantized vortices may be created in some metastable state, long-lived enough to be detected. However, the question of whether ^4He droplets can sustain vortices is still not resolved, and all the high resolution spectra of embedded molecules can apparently be explained without invoking their presence. Yet, it is expected that in the near future they could be created by some extension of the present experimental techniques. This calls for identifying signatures that might reveal vortical states in helium droplets. A possible experiment to detect their presence has been described by Close *et al.* [3]. They have suggested that alkali atoms, that normally reside in a “dimple” on the surface of ^4He clusters [6–8], may be drawn, when a vortex is present, *inside* the cluster along the vortex core. Spectroscopic experiments on the dopant atoms could thus provide evidence of their existence, since the line broadenings and shifts would be different in the two cases. We show in the following that alkali atoms are actually not suited for such an experiment, but rather alkaline earth (Ca) atoms may serve as probes to detect vortices.

Density functional (DF) methods [9] have become increasingly popular in recent years as a useful computational tool to study the properties of classical and quantum inhomogeneous fluids, especially for large systems, for which they provide a good compromise between accuracy and computational cost. In particular, a quite accurate description of the properties of inhomogeneous liquid ^4He at zero temperature has been obtained within a

DF approach by using the energy functional proposed in Ref. [10] and later improved in Ref. [11]. This later DF, which has been successfully used over recent years to study a variety of ^4He systems such as clusters and films, is the one we use in the present work.

The minimization of the energy functional with respect to density variations, subject to the constraint of a given number of ^4He atoms N , leads to the equilibrium particle density profile $\rho(\mathbf{r})$, thus allowing us to study the static properties of the ^4He system. When dynamical properties are studied (as described in the following), we use the time-dependent DF (TDDF) method developed in Ref. [12], which allows us to obtain both the ^4He particle density $\rho(\mathbf{r}, t)$ and the velocity field $\mathbf{v}(\mathbf{r}, t)$. Briefly, in the static (dynamic) case, one has to solve a stationary (time-dependent) nonlinear Schrödinger-like equation for an “order parameter” $\Psi(\mathbf{r})$ [$\Psi(\mathbf{r}, t)$], where the Hamiltonian operator is given by $H = -\frac{\hbar^2}{2m}\nabla^2 + U[\rho, \mathbf{v}]$. The effective potential U is defined as the variational derivative of the energy functional, and its explicit expression is given in Ref. [12]. From the knowledge of $\Psi \equiv \phi e^{i\Theta}$, one can get the density $\rho(\mathbf{r}, t) = \phi^2$ and the fluid velocity field $\mathbf{v}(\mathbf{r}, t) = \frac{\hbar}{m}\nabla\Theta$. To model the interaction of liquid ^4He with foreign impurities, we use suitable He-impurity pair interaction potentials, which will be described later on.

We work in 3D Cartesian coordinates, and adopt the following procedure to generate a vortex in the cluster in the most unbiased way. We consider a cluster in a rotating frame of reference with constant angular velocity ω_z around the z axis [13]. The Hamiltonian density H then acquires an additional term $-\omega_z \hat{L}_z$, \hat{L}_z being the angular momentum component along the z axis. We minimize Ψ for this constrained Hamiltonian, imposing Ψ to be orthogonal, during the minimization, to $\Psi_0 = \sqrt{\rho_{eq}}(\mathbf{r})$ describing the minimum energy state of the vortex-free cluster; we have applied the method to a $N = 300$ droplet. To generate a vortex line, ω_z must be larger than a critical value—unknown in advance— $\Omega_c = \Delta E/(N\hbar)$ [14],

where ΔE is the energy cost to create a vortex (which in the present case is about 70 K, see Table I, and, hence, $\Omega_c \sim 3 \times 10^{10} \text{ s}^{-1}$), but not so large that one could generate a vortex array [13]. The particle density corresponding to this vortical configuration is shown in Fig. 1(a). We have calculated the circulation of the velocity field along a path enclosing the vortex core, and have exactly found the value Nh/m appropriated for a quantized vortex with $\langle \hat{L}_z \rangle = N\hbar$.

Note that, since the vortex is quantized, the vortical state is an eigenstate of the angular momentum along the rotation axis, \hat{L}_z . This means that our density profile is the same as what one would obtain by using the Feynman-Onsager ansatz, i.e., by adding to the energy functional an extra centrifugal term associated with an order parameter of the form $\sqrt{\rho}e^{i\Phi}$ (Φ being the azimuthal angle), and finding the density profile by solving an equation in the real quantity $\sqrt{\rho(\mathbf{r})}$. This is the procedure used in the DF calculations of Ref. [5] to generate quantized vortex structures in helium drops—and also in Bose-Einstein condensates of trapped gases [14]. Instead, we have not assumed *a priori* a quantized value for the total angular momentum, but rather we generate a fully quantized vortex state starting from a pure cluster.

To use atomic impurities as probes of the presence of vortices in ^4He drops, ideally one would like to have an atom that is *barely* stable on the surface of a pure drop, and becomes solvated in its interior in the presence of a vortex. The question of solvation vs surface location for an impurity atom in liquid ^4He can be addressed in an approximate way within the model of Ref. [15] where, based on calculations of the energetics of impurities interacting with liquid ^4He , a simple criterion is proposed to decide whether surface or solvated states are favored. An dimensionless parameter is defined in terms of the impurity-He potential well depth ϵ and the minimum position r_m , $\lambda \equiv \rho \epsilon r_m / (2^{1/6} \sigma)$, where ρ and σ are the bulk liquid density and surface tension of ^4He , respectively. The criterion for solvation reads $\lambda > 1.9$ for the

TABLE I. Energies of several $^4\text{He}_{300}$ configurations. In the left part of the table, they are referred to the total energy of the pure, vortex-free cluster (-1384.5 K), whereas in the right part they are referred to that of the cluster + vortex configuration (-1313.4 K). The configurations marked with an asterisk are unstable stationary configurations.

Configuration	E (K)	Configuration	E (K)
Rb (center)*	+94.7	Rb/vortex (center)*	+71.7
Rb (top)	-9.1	Rb/vortex (top)	-12.5
Na (center)*	+64.3	Na/vortex (center)*	+45.1
Na (top)	-8.1	Na/vortex (top)	-11.3
Ca (center)*	-33.7	Ca/vortex (center)	-49.9
Ca (top)	-37.4	Ca/vortex (top)	Unstable
Vortex	+71.1		

existence of solvated states [15]. One thus needs an impurity with $\lambda \sim 2$, and such that its most stable state is on the drop surface.

Alkali atoms are known to have their stable state on the surface of liquid ^4He [6,7], and they lie in the low λ regime ($\lambda \sim 0.6-0.9$) [15]. Accordingly, for alkalis a surface state should always be preferred, even in the presence of a vortex line. We have verified this point considering Na and Rb, as representative of a light and a heavy alkali, respectively. The alkali-He interaction is of the form proposed by Patil [16]. We have compared the stable dimple states of Na and Rb atoms on the surface of the $N = 300$ cluster hosting a vortex line, with those of the same impurity trapped in the vortex core, exactly at the cluster center. We have found that the latter are energetically unfavored with respect to surface states (see Table I). It is worth noting that, in the case of Na, our results compare well with the path integral Monte Carlo calculations of Ref. [17], where a binding energy of about ~ 7 K is found for this cluster. We also note that, unlike the case of strongly bound impurities to ^4He clusters [5], which have their stable state inside the cluster, and for which there exists a critical cluster size below which the droplet + dopant + vortex complex is stable, the alkalis cannot stabilize the vortex, whatever the droplet size [5].

There are other dopants, however, for which there is clear evidence of a surface state on liquid ^4He , i.e., alkaline earth atoms. Absorption spectra of alkaline earth atoms (Ca, Ba, and Sr) attached to ^4He clusters clearly support an outside location of Ca and Sr [18], and probably also of Ba [19]. To describe the He-impurity interaction, we employ an accurate *ab initio* He-Ca pair potential [20] used to study $^4\text{He}_N + \text{Ca}$ droplets up to $N = 75$ by diffusion Monte Carlo techniques [21]. For such a potential, $\lambda \sim 2.2$, which apparently indicates a solvated stable state. However, for those cases where λ is close to the solvation threshold, consideration of the shape of the potential energy surface, as well as the well depth and equilibrium internuclear distance, seems warranted [22].

The stable state of a Ca atom in a $^4\text{He}_{300}$ vortex-free cluster is shown in Fig. 1(b). Note that, in qualitative agreement with the experimental evidence, the dimple

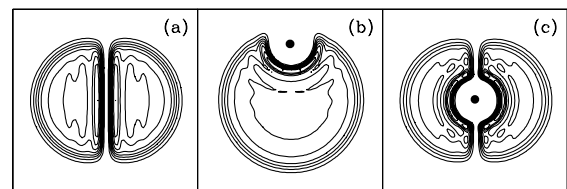


FIG. 1. From left to right, for a $^4\text{He}_{300}$ cluster, atomic density lines corresponding to (a) the vortical state, (b) the deep dimple stable state of Ca, and (c) the solvated stable state of Ca in the presence of a quantized vortex. Each box side has 45 \AA length.

appears to be much more pronounced than in the case of alkalis [12], reflecting the stronger He-atom interaction. However, in the presence of a vortex, the stable state is in the center of the cluster, as depicted in Fig. 1(c). The surface state in this case is unstable and, as the minimization proceeds, a Ca atom initially placed on the surface near the vortex core is gradually drawn towards it and then sucked inside, eventually reaching the stable state in the center of the drop. The value of the angular momentum for the converged ${}^4\text{He}$ configuration is again $\langle \hat{L}_z \rangle = N\hbar$.

The response of the impurity atom to the different ${}^4\text{He}$ environments shown in Fig. 1 might be determined with spectroscopic measurements, allowing one to detect the presence of vortices: The observed linewidths and shifts of the excitation/emission spectra in the two cases shown in Fig. 1 should be very different, reflecting the “bubble” environment in one case [Fig. 1(c)], and a more open environment in the other case [Fig. 1(b)]. Moreover, in the case of Fig. 1(b), bound-unbound transitions should be observed with a significant probability, thus implying a strong asymmetry in the observed spectra.

In the above picture, one is assuming that the vortex is long-lived enough to allow a Ca atom, picked up randomly by the cluster, to diffuse close to the top of the vortex core and then to be drawn inside. We have no direct proof of the stability of the cluster + vortex complex on experimental time scales. However, we have indications that the cluster + vortex + dopant complex should be stable at least on the nanosecond time scale. This conclusion comes from very long computing time simulations, using the TDDF method [12], to study the dynamics of the cluster + vortex + impurity complex. During these simulations, the impurity atoms were allowed to oscillate inside the bubble in the cluster center [see Fig. 1], and the vortex line was always found to be stable, without showing any tendency to shrink, bend, or migrate towards the surface of the cluster.

The solvated state for Ca in a vortex-free cluster is a stationary but unstable configuration against any displacement of the atom off the cluster center, only a few K in energy above the stable, dimple state (see Table I). This is a consequence of the borderline value of λ for this impurity and implies that, in a real experiment, a fraction of Ca atoms might be trapped inside the clusters for fairly long times, even in the absence of vortices. For these atoms, the spectroscopic signals would be similar to those coming from Ca atoms trapped in the vortex core, making it difficult to discriminate between the two cases. A line shape calculation [6] using as an input the ${}^4\text{He}$ density profiles around the impurity might help to distinguish between solvated states of Ca with and without vortex. Since the extension of the method of Ref. [6]—which is applied there to the simpler case of the mono-electronic alkali atoms—is rather involved for two-electron systems, we have not carried out such a calcu-

lation. We instead suggest additional measurements which may help to discriminate between the states shown in Fig. 1.

It appears from our calculations that the energy of the impurity-cluster system is rather insensitive to the location of Ca along the vortex core, once the atom is embedded in it. Consequently, vibrational modes of the impurity along the vortex line are expected to be soft. We have confirmed this by TDDF calculations, applying to the Ca atom a small initial momentum in a given direction, radially, towards the surface of the cluster for the dimple state of Fig. 1(b), and along or perpendicular to the vortex line in the case shown in Fig. 1(c). We then let the impurity evolve in time, allowing for the ${}^4\text{He}$ environment to dynamically follow the atom motion while the impurity oscillates around its equilibrium position. This is done in practice by numerically solving by means of a discrete Verlet algorithm, as is usually done in molecular dynamics calculations, Newton’s equation of motion for the Ca atom under the force due to the surrounding ${}^4\text{He}$ liquid:

$$M \frac{d^2 \mathbf{R}}{dt^2} = -\nabla_{\mathbf{R}} \left\{ \int \rho(\mathbf{r}, t) V_{\text{He-Ca}}[\mathbf{R}(t) - \mathbf{r}] d\mathbf{r} \right\}.$$

In this expression, $V_{\text{He-Ca}}$ is the pair potential describing the He-impurity interaction, and the density $\rho(\mathbf{r}, t)$ is updated at each time step according to the TDDF scheme for ${}^4\text{He}$ [12]. From the positions of the Ca atom as a function of time, relative to the center of mass of the Ca-He droplet system, different frequencies characterizing the impurity dynamics can be found from a Fourier analysis of the calculated time series.

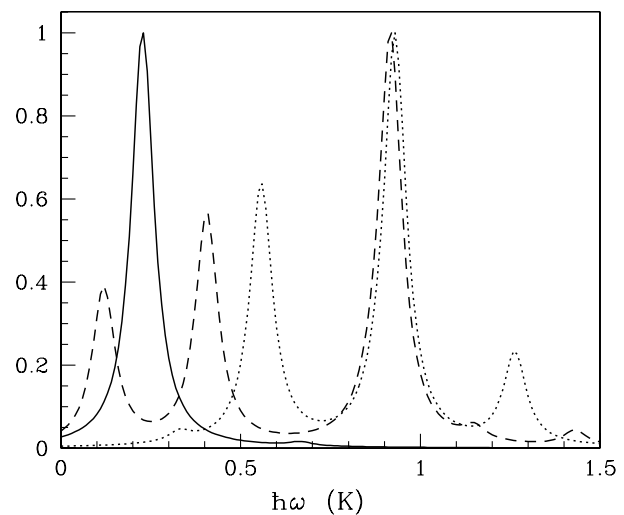


FIG. 2. Calculated frequency spectra for the oscillations of a Ca atom in a ${}^4\text{He}_{300}$ cluster. Solid line: Solvated state [see Fig. 1(c)], Ca moving along the vortex core; dashed line: solvated state, Ca moving perpendicular to the vortex core; dotted line: surface state [see Fig. 1(b)], Ca moving in the radial direction.

We report in Fig. 2 the calculated vibrational spectra. The intensities are in arbitrary units, and normalized so that the higher peak in each spectrum has unit height [23]. It appears that the oscillation of Ca along the vortex core is indeed characterized by a single low frequency mode, as compared with the more fragmented spectrum for vibrations perpendicular to the vortex core. The presence of the soft mode is a signature of solvation of a Ca atom inside the vortex. Indeed, such a mode should be severely damped, or even absent, for a solvated Ca atom in a vortex-free cluster, since this configuration is unstable. We also show for comparison the vibration spectrum of a Ca atom in the dimple state on the surface of a cluster without vortex. The peak just below 1 K is due to the “dipolar” vibration of the impurity inside the semi-spherical (spherical) cavity in which it is trapped in the dimple (bubble) state. Additional peaks appear in the dimple spectra because of the coupling of the Ca motion with the surface modes of the ^4He nanodroplet, which have similar frequencies (for instance, the lowest energy, $l = 2$ quadrupolar mode of a pure $^4\text{He}_{300}$ droplet occurs at ~ 0.6 K [12]). All these modes lie in the microwave frequency regime, and there are experimental ideas to measure the corresponding vibrational frequencies [24].

It is worth seeing how these modes are coupled, which is particularly apparent when we displace the impurity perpendicular to the vortex core (dashed line in Fig. 2). To trigger this oscillation, we have given to the impurity a kinetic energy of about 2 K, 3 times as much as in the other two cases. One may see that the spectrum displays one peak corresponding to the dipolar mode discussed previously, and also softer modes of characteristics similar to those found in the other two cases. This coupling is possible because the time evolution is adiabatic.

Finally, we emphasize that the dynamical behavior of He-impurity systems depends in a sensitive way on the details of the He-atom pair interaction. This calls for improving the available interaction potentials to strengthen the scenario described here, or to help in finding other atomic/molecular impurities which may serve as probes of the presence of vortices in ^4He droplets.

We thank M.W. Cole, F. Dalfovo, W. Ernst, S. Hernández, G. Scoles, F. Stienkemeier, and F. Toigo for useful comments and discussions. We thank Professor W. Meyer for the permission of using his unpublished Ca-

He potential. F. A. acknowledges funding from MIUR-COFIN 2001 (Italy), and M. B. and M. P. from BFM2002-01868 and 2001SGR00064 (Spain).

-
- [1] J. P. Toennies and A. F. Vilesov, *Annu. Rev. Chem.* **49**, 1 (1998); K. K. Lehmann and G. Scoles, *Science* **279**, 2065 (1998).
 - [2] C. Callegari *et al.*, *Phys. Rev. Lett.* **83**, 5058 (1999); **84**, 1848(E) (2000); Y. Kwon *et al.*, *J. Chem. Phys.* **113**, 6469 (2000); E.W. Draeger and D.M. Ceperley, *Phys. Rev. Lett.* **90**, 65301 (2003).
 - [3] J. D. Close *et al.*, *J. Low Temp. Phys.* **111**, 661 (1998).
 - [4] G. H. Bauer, R. J. Donnelly, and W. F. Vinen, *J. Low Temp. Phys.* **98**, 47 (1995).
 - [5] F. Dalfovo *et al.*, *Phys. Rev. Lett.* **85**, 1028 (2000); R. Mayol *et al.*, *ibid.* **87**, 145301 (2001).
 - [6] F. Stienkemeier *et al.*, *Z. Phys. D* **38**, 253 (1996).
 - [7] F. Ancilotto *et al.*, *Z. Phys. B* **98**, 323 (1995).
 - [8] F. Stienkemeier *et al.*, *J. Chem. Phys.* **102**, 615 (1995); C. Callegari *et al.*, *J. Phys. Chem. A* **102**, 95 (1998).
 - [9] R. Evans, *Adv. Phys.* **28**, 143 (1979).
 - [10] J. Dupont-Roc *et al.*, *J. Low Temp. Phys.* **81**, 31 (1990).
 - [11] F. Dalfovo *et al.*, *Phys. Rev. B* **52**, 1193 (1995).
 - [12] L. Giacomazzi, F. Toigo, and F. Ancilotto, *Phys. Rev. B* **67**, 104501 (2003).
 - [13] R. J. Donnelly, *Quantized Vortices in Helium II* (Cambridge University Press, Cambridge, England, 1991).
 - [14] F. Dalfovo and S. Stringari, *Phys. Rev. A* **53**, 2477 (1996).
 - [15] F. Ancilotto, P. B. Lerner, and M.W. Cole, *J. Low Temp. Phys.* **101**, 1123 (1995).
 - [16] S. H. Patil, *J. Chem. Phys.* **94**, 8089 (1991).
 - [17] A. Nakayama and K. Yamashita, *J. Chem. Phys.* **114**, 780 (2001).
 - [18] F. Stienkemeier, F. Meier, and H. O. Lutz, *J. Chem. Phys.* **107**, 10 816 (1997).
 - [19] F. Stienkemeier, F. Meier, and H. O. Lutz, *Eur. Phys. J. D* **9**, 313 (1999).
 - [20] W. Meyer (private communication).
 - [21] M. Lewerenz (unpublished).
 - [22] J. Reho *et al.*, *J. Chem. Phys.* **112**, 8409 (2000).
 - [23] We have added to the bare spectra a Lorentzian broadening of width $\Delta\omega \sim 2\pi/t_{\text{max}}$, which reflects the finite duration of our simulations, $t_{\text{max}} \sim 0.5 \times 10^{-9}$ s.
 - [24] W. Ernst (private communication).